Rain-induced variability of near sea-surface T and S from drifter data

Gilles Reverdin, Simon Morisset, Jacqueline Boutin, Nicolas Martin

Rain-induced variability of near sea-surface T and S from drifter data

G. Reverdin,[1] S. Morisset,[1] J. Boutin,[1] and N. Martin[1]

Received 25 August 2011; revised 6 December 2011; accepted 11 December 2011; published 22 February 2012.

[1] The effect of rain on sea surface temperature, salinity and density is examined using data of surface drifters in regions of the tropical oceans with large rainfall. In a few off-equatorial areas, there are sufficient drifter data to composite average daily cycles. There, the period of the day with largest salinity changes is associated with the largest rainfall rates and the lowest salinity. For a one-yearlong trajectory in the southwest Pacific, this results in an early morning salinity minimum, whereas the opposite is found close to equatorial West Africa. We then consider individual freshening events larger than 0.1 psu (averaging 0.56 psu at 50 cm), and find that they are often related with local rainfall, are associated with a surface cooling, and relax in a time inversely proportional to wind intensity. The temperature cooling is dependent on the time of day, but the freshening presents less daily cycle and the largest fast changes in salinity tend to be associated with the largest rainfall rates. When two measurement levels are available, the initial salinity signal is larger by more than 20% at the shallow depth (15 cm) compared with the deeper measurement level (near 50 cm), and the temperature and salinity gradients between the two levels are proportional (0.22°C for a 1% dilution).

Citation: Reverdin, G., S. Morisset, J. Boutin, and N. Martin (2012), Rain-induced variability of near sea-surface T and S from drifter data, *J. Geophys. Res.*, *117*, C02032, doi:10.1029/2011JC007549.

1. Introduction

[2] Salinity has been monitored over the world oceans with near sufficient sampling since the mid-2000s to evaluate global or regional budgets on seasonal time scales, in particular with the advent of the ARGO profiler array [*Roemmich et al.*, 2009; *von Schuckmann et al.,* 2009; *von Schuckmann and Le Traon*, 2011; *Willis et al.*, 2009, and references therein; *Johnson and Wijffels*, 2011]. Numerous studies have indicated that the near surface salinity spatial contrasts have intensified during the last fifty years, the fresh regions tending to get fresher, and the salty regions tending to get saltier [*Schmitt*, 2008; *Gordon and Giulivi*, 2008; *Delcroix et al.*, 2007; *Cravatte et al.*, 2009; *Durack and Wijffels*, 2010], possibly as a result of an intensification of the freshwater cycle [*Yu*, 2007]. Thus part of the change in freshwater budget is likely to be contained in the near surface layers of regions with excess rainfall or excess freshwater input through river or ice-melt, which are often very stratified near the surface (often with barrier layers in the tropical oceans, as described for example by *Lukas and Lindstrom* [1991], *Sprintall and Tomczak* [1992], *Mignot et al.* [2007], and *Tanguy et al.* [2010]). These regions are highly spatially variable and thus are not so well sampled by the current monitoring systems. This was one motivation (in particular for the tropical oceans) for the launch of L-band microwave satellite missions in the last few years (SMOS from ESA in October 2009 [*Font et al.*, 2010, 2012], and AQUARIUS from NASA/CONAE in June 2011 [*Lagerloef et al.*, 2010; *Le Vine et al.*, 2010]). The satellite measurements are sensitive to salinity in the top cm of the ocean. They need to be validated, which in areas of excess freshwater input, is not that easy with other measurements often at a few meters below the surface. *Henocq et al.* [2010] have shown statistically that salinity was increasing between 1-m depth and 5 to 10-m depth within all tropical regions where rainfall dominates. The salinity difference with the uppermost reliable measurement of ARGO floats typically at a 5-10-m depth thus increases as one gets closer to the sea surface. *Henocq et al.* [2010] also indicate that the vertical gradients tend to correlate with rainfall within the previous three days.

[3] There are few reported examples of response to local intense rainfall close to the sea surface [*Katsaros and Buettner*, 1969; *Vialard et al.*, 2009], because there were few instrumental devices deployed to measure in the top few meters of the ocean. *Price* [1979] and *Wijesekera et al.* [1999] have shown the relatively fast vertical spreading to depths of 10 m or more over a few hours to a day in typical intense equatorial Pacific rain events. They also show how simultaneously some of this freshwater spreads away from its source, advected by the currents. A budget was also carried from moorings in TOGA COARE [*Cronin and McPhaden*, 1998], which indicates how quickly the near surface-trapped signals (their first sensor was 1 m below the surface) propagate deeper to

[1]Laboratoire d'Océanographie et de Climatologie par Expérimentation et Analyse Numérique, Institut Pierre Simon Laplace, CNRS/UPMC/IRD/MNHN, Paris, France.

0148-0227/12/2011JC007549

10 m or more, to a good extent because of the relatively large winds and vertical mixing that are associated with most of the large rain events in the western equatorial Pacific. These results were later extended to other areas with large rainfall and with similar results (M. McPhaden, personal communication, 2011). *Soloviev and Lukas* [1997] have also shown how the spreading of freshwater lenses induced by rainfall is sometimes associated with intensified surface fronts, probably as bores in some instances, inducing sudden salinity changes across horizontal distances as small as 10 m, and this away from direct rainfall, and at latitudes that can exceed 10° of the equator.

[4] The daily cycle of surface (1m depth) salinity was investigated from a mooring in the western equatorial Pacific [*Cronin and McPhaden*, 1999], in a region where average rainfall is large. It showed that although rainfall peaked there in the late night-early mooring, the minimum salinity was in the afternoon, and there was a maximum (by 0.1 psu) in the late night. They attribute this average effect to intensified nighttime mixing with saltier subsurface water, counteracting the excess nighttime rainfall freshening. To a large extent, these results apply to other sites of the TAO-PIRATA-RAMA mooring arrays (M. McPhaden, personal communication, 2011), although a full synthesis still needs to be established.

[5] Here, we will for the first time use surface drifters measuring temperature and salinity to investigate the response of the surface layer to tropical rainfall events. One advantage of drifters is the possibility to measure closer to the surface (typically near 50 cm), and with less perturbation of the surface layer by the instrument than for moored instrumentation. We will also be able for the first time to investigate stratification in the 15 to 50 cm layer. Also, the drifter provides a quasi-Lagrangian view (the drifters used in this study are drogued at 15 m), though we expect during a rain event to have relative flow of the near-surface fresh layer relative to the drifter. We will specifically explore off-equatorial areas of the Inter Tropical Convergence Zone (ITCZ) and South Pacific Convergence Zone (SPCZ), that might exhibit a different response than the equatorial site studied by *Cronin and McPhaden* [1999]. In section 2, we will present the drifters and the characteristics of the data used. In section 3.1, we will present statistical characteristics of the variations in near-surface salinity associated with rainfall, and the average daily cycle observed. In sections 3.2 and 3.3, we will investigate the near-surface response associated to individual short-term rain events, and section 4 is a discussion-conclusions section.

2. Data Sets

2.1. Drifters

[6] The drifters are SVP-BS models manufactured by Pacificgyre and Metocean [*Reverdin et al.*, 2007]. They have an unpumped SBE37 C/T unit and an additional SST measurement along the float's hull near 18 cm. Since the work by *Reverdin et al.* [2007], the main changes have been to move the temperature sensors closer to the conductivity cells, change the conductivity cell in Metocean drifters (now identical to the one in the Pacificgyre drifter, and placed vertically), and increase the resolution in reported T. Some of the recent Metocean drifters used Iridium data transmission (and GPS positioning) and have a higher T resolution on the order of 0.01°C. Salinity is reported at regular intervals with a resolution on the order of 0.01 pss-78 (practical salinity scale, according to the 1978 practical salinity scale; for simplification in the following, we will use the notation 'psu' for salinity values) on all these drifters, and the data correspond to an average of individual values over a relatively short period (a few minutes). The presence of the drogue was usually sensed unambiguously, except during periods of low winds. Most drifters of this study have retained their drogue.

[7] We also use additional data from a small conductivity cell (manufactured by ASD Sensortechnik GmbH) placed 15 cm below the sea surface under a small Surplas float (with associated T measurement 2 cm below the cell; see an earlier version of the float in the work by *Reverdin et al.* [2007]). The float is loosely tethered to the SVP-BS drifter. The measurements are every 15 min corresponding to the median of data over 8 s and reported at roughly 0.001 psu/0.01°C resolution in S/T. The measurement autonomy is between 1 month and 2 months, but the conductivity sensor is quickly bio-fouled with on the order of 1 month of recoverable data. The combination of these data with the SVP-BS data can be used to estimate near-surface stratification.

[8] The drifters we consider in this study were all deployed in the tropical oceans in 2007–2010 with data until February 2011, mostly in regions of high rainfall and fairly low salinity (Figure 1), although portions of these trajectories correspond to the dry season with little reported rainfall (usually with higher salinities). These include two short trajectories in the Indian Ocean, some trajectories in the southwestern Pacific, including a long one (92546, plotted separately in Figure 1b), and trajectories in the central or western tropical Atlantic Ocean.

2.2. Data Processing

[9] The reported T/S data of SVP-BS drifters are checked for transmission/electronics errors (isolated point check in T/S). Suspicious spikes are removed, usually mid-day data during very strong daily cycles of temperature (larger than 0.8°C amplitude), which are examined systematically to check the presence of S biases that would result in mismatch between the conductivity cell temperature and the measured temperature [see *Reverdin et al.*, 2007] (although changes in temperature sensor position have recently diminished the problem). The data are then checked for suspicious jumps that could indicate that an object got stuck in the conductivity cell. A jump larger than 0.1 psu in S with no associated jump (larger or equal to 0.05°C) in T is considered suspicious, if there is no gradual recovery during the following 24 h (examples in Figure 2a). These jumps are most commonly toward lower values, but can be followed by jumps toward higher values. The parts affected by the jumps are removed from further analysis, although we know from paired SVP-BS/Surplas drifters that such jumps are not always erroneous.

[10] Then the salinity data are compared with co-localized Argo floats (less than 100 km and 2 days from the drifter) to check for possible drifts. This was not easy to apply in the high variability region of the western equatorial Atlantic, except for identifying periods in which the sensor was too fouled to be of any use, in which case the data were removed. Otherwise, collocated ARGO data are used to correct drifts/biases larger than a few 0.01 psu, which do not seem to be

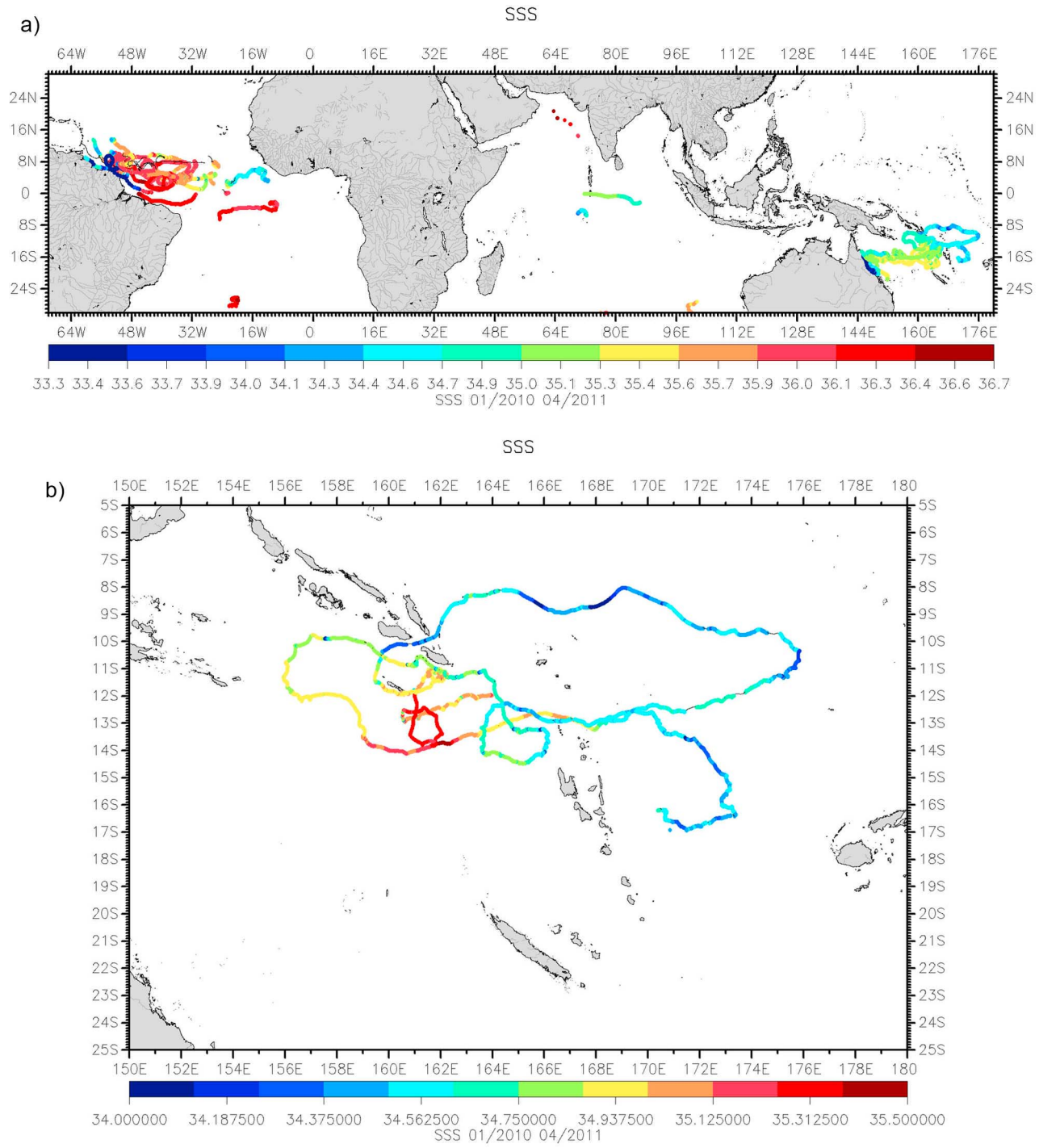

Figure 1. Map of the salinity drifter trajectories used in this study. The drifter trajectories are color-coded according to salinity. (a) All the trajectories and (b) the trajectory of SPP-BS 92546.

very common, at least at midlatitudes when they can be ascertained. In the wet tropics, this is much harder, due to high temporal/spatial variability as is illustrated for drifter 92546 located in the southwestern Pacific near the South Pacific Convergence Zone (SPCZ) (Figure 2b), and possible biases of up to 0.1 psu could still be present on parts of the record.

[11] The Surplas S and T records were then adjusted to collocated SVP-BS S and T data. We first remove spikes (outliers) due to erroneous transmission (as was done for SVP-BS drifters, but these are more frequent on Surplas data). Then, we shift the reported time of the Surplas data to the one of the SVP-BS drifter by lag-correlations of interpolated records during periods of low vertical stratification (usually for periods with no rain during evening-night).

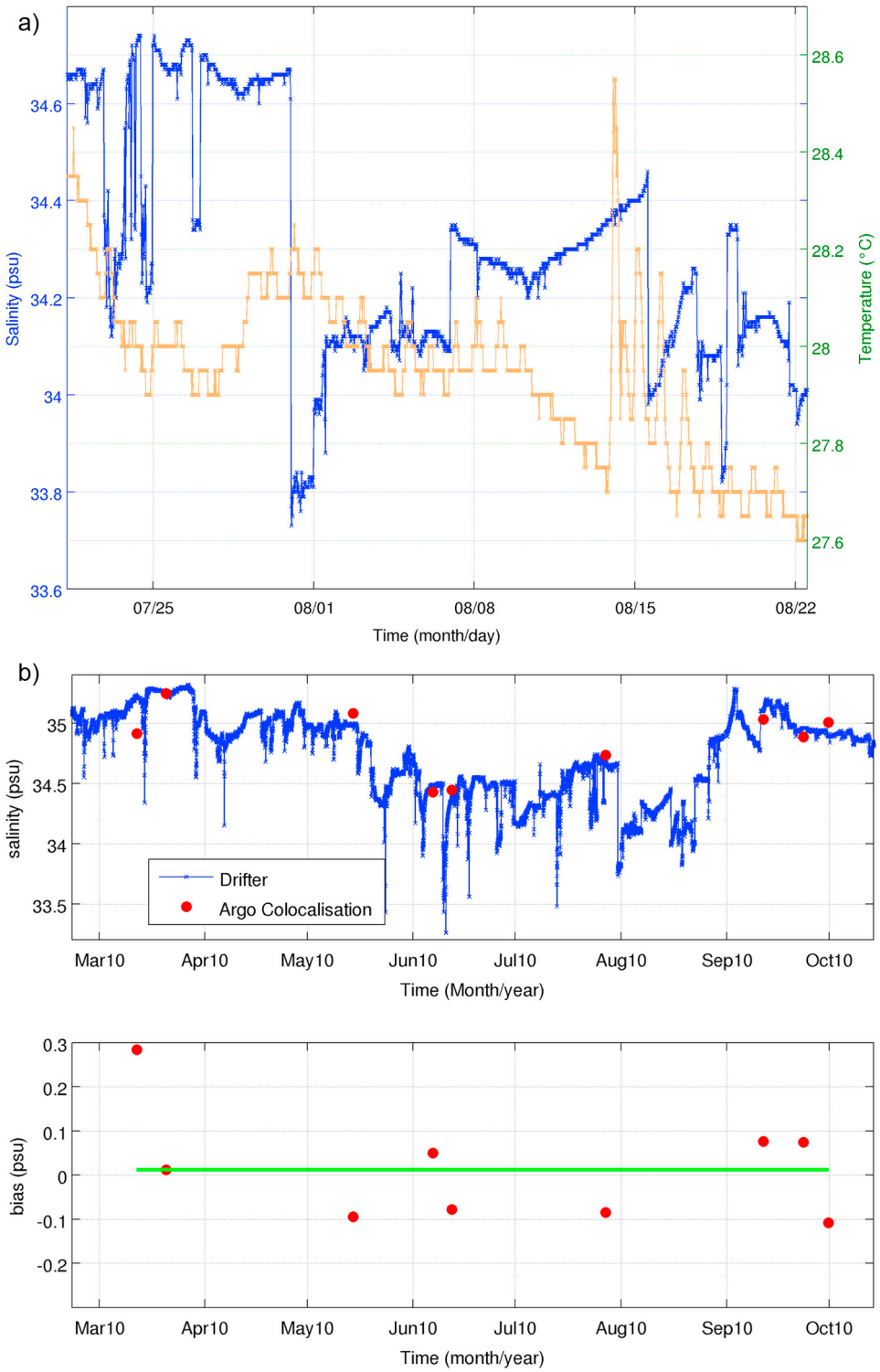

Figure 2. (a) Example of T and S records between July 22 and August 22 2010 for Pacificgyre drifter 92546 (S in blue and T in green). (b) (top) The 'original' salinity time series collocated with Argo float data at their uppermost level and (bottom) the difference of the two together with the average estimated bias (horizontal line). Notice that the data in Figure 2b (top) have not been filtered with a few positive spikes in mid-day during days with very large SST mid-day warming.

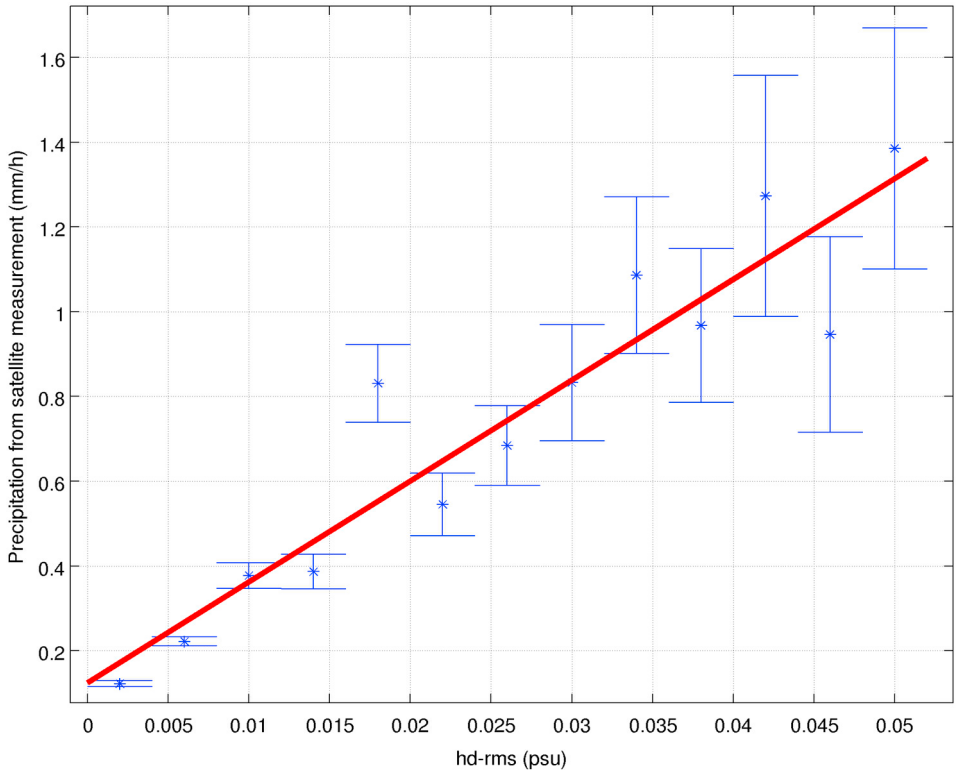

Figure 3. Average rainfall (mm/hour) as a function of 3-h RMS of the changes in salinity during 30′ (hd-rms; psu). Only times when rainfall is reported are retained for a one-year segment (February 2009-January 2010) of drifter 92546 deployed in the southwest tropical Pacific Ocean. The data are sorted in classes of hd-rms and the error bars are plotted on the average rainfall.

These time shifts can reach up to 15 min. Then, because of important fouling of the Surplas C-cell, we adjust on a nearly daily basis the Surplas S data to the SVP-BS S by comparing periods when there is no time variability associated with rain or crossing of fronts. We find that the useful part of the Surplas record is often on the order of a month or so in the water, although this has varied greatly between drifters. For the comparisons presented later, the Surplas data are linearly interpolated to the time of the less-frequent SVP-BS measurement.

2.3. Satellite Retrievals

[12] Rain rate and wind speed retrieved from various satellite microwave radiometer missions (www.ssmi.com) have been co-located with the drifter data. This includes data from the Special Sensor Microwave Imager (SSM/I) aboard two polar-orbiting satellites (F15 and F16) [*Wentz and Spencer*, 1998], the Tropical Rainfall Measuring Mission (TRMM) Microwave Imager (TMI) and the Advanced Microwave Scanning Radiometer (AMSR-E). The spatial resolution of the rain-rate retrievals is variable between these different satellite missions, because of the different instrument and processing characteristics, but is never less than 20 km and the data are reported on a 1/4° grid. The accuracy of the retrievals is also variable, with biases of up-to-20% possible between different satellite missions [*Gruber and Levizzani*, 2008]. There are typically between 8 and 10 instantaneous co-located rain rate data for each day at irregular intervals. We also use the microwave wind speed data, although wind speed is not retrieved during heavy rainfall.

[13] There has been ample discussions on daily cycle of precipitation over the tropical oceans from these different satellite data sets [*Chang et al.,* 1995; *Yang and Smith*, 2006; *Kikuchi and Wang*, 2008; *Rauniyar and Walsh*, 2011], indicating that in large parts of the deep-convective tropics, there is a maximum of rainfall in the late night–early morning. This holds particularly under the regions and periods of large convective activity (for example, the ITCZ or SPCZ, away from continents).

3. Results

3.1. Salinity Fast Variability and Daily Cycles

[14] To characterize fast salinity changes, we chose the three-hourly RMS variability of the time series of S change between successive values (30′ apart) (noted as hd-rms). We compare those to rainfall rates, by pairing a hd-rms value to each rainfall event in the co-located rain rates. The rain rates are then bin-composited as a function of hd-rms (Figure 3). This indicates for this long-lived drifter under the SPCZ (SVP-BS 92546) a nearly linear relation between hd-rms and rain rate, when rain is reported. Other drifters in different tropical regions, indicate similar relationships (roughly 1.3 mm/hour for 0.05 psu in hd-rms). We find no statistical dependence of this relationship with the time of day (separating nighttime and day-time). Notice also the large uncertainty for

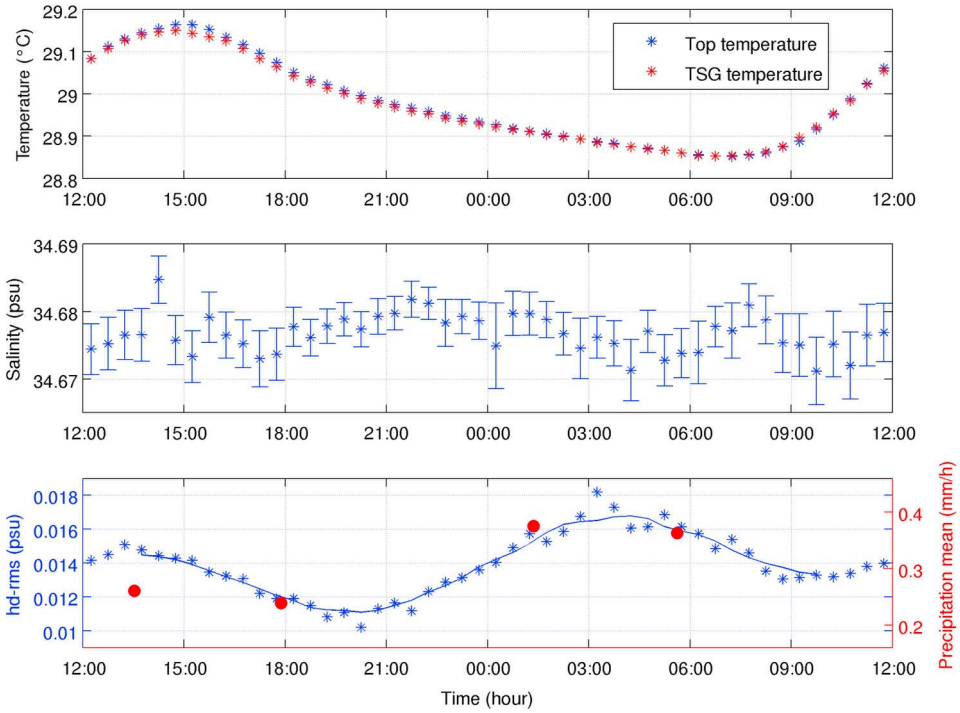

Figure 4. Average daily cycle for drifter SVP-BS 92546 in the southwest Pacific (February–July 2009 and November–January 2010 to only consider the most rainy season). Time is in local time. (top) T at two levels (blue, upper hull-measurement near 15–20 cm of the surface; red, measurement near 50 cm associated with the C/T cell); (middle) average salinity daily cycle (only days with no front crossed and no large SST daily cycle (>1°C) are retained, and the estimated RMS error is plotted), and (bottom) hd-rms (blue dots) and rainfall (red points). In Figure 4 (bottom), the blue line is a 3-h running average of the half-hourly values.

the large hd-rms categories. This is only partially explained by the dependency of uncertainty on sample size (on the order of 250 and 100 for hd-rms categories of 0.02 and 0.035, but 3000 for hd-rms of 0.000, 0.005 and 0.010). We also expect a larger scatter in the ocean surface salinity during intense rain events associated with the wind conditions, and thus the induced vertical mixing.

[15] For drifter SVP-BS 92546 near the Southwest Pacific SPCZ, this fast variability of SSS (hd-rms) presents an average daily cycle with a minimum in the late afternoon and a maximum in the late night, thus a range in daily cycle of 40% of its average value (Figure 4). The average rainfall for the 4 daily SSM/I observations in this area of high average rainfall (SPCZ) indicates rainfall twice as large in the early morning than in the afternoon (confirmed by the other co-located rainfall satellite data). This in phase dependency is consistent with the observed dependency between hd-rms and rain rate data, when rainfall is reported, presented in Figure 3. Although rain only occurs 16% of the time for SVP-BS 92546, hd-rms is smaller when it does not rain, and thus does not influence much the daily cycle in Figure 3 (we have removed days when the drifter crossed large fronts before compositing).

[16] For drifter SVP-BS 92546, the average salinity daily cycle presents a weak morning minimum, and thus differs from the instantaneous rainfall rates and hd-rms cycle (Figure 4). The peak-to-peak amplitude of an average daily cycle is less than 0.01 psu. Except near 15:00 local time, there is no average vertical temperature gradient, so the mismatch in thermistor and conductivity cell depths should not have affected the estimated S between 6:00 P.M. and 12:00 A.M. On the other hand, it could have led to a slight overestimate of S between 12 A.M. and 6 P.M. The daily cycle observed is a little smaller than for the equatorial mooring data given by *Cronin and McPhaden* [1999], where a salinity daily cycle was found with a minimum in the late afternoon.

[17] We checked the daily cycle for other drifters in high precipitation regions (and seasons). However, the time series were not long enough to estimate a significant daily cycle. A special case is for drifter SVP-BS 54175 often to the west of Guinea in West Africa, in a region of very large rainfall. In this case (Figure 5), hd-rms and rainfall were much larger in the afternoon/early night (12 A.M. to 9 P.M.), with resulting larger uncertainty on the lower SSS at those times. There is nevertheless in this case a large daily cycle. Near 3 P.M., the S values for this drifter could be slightly too large as a result of positive temperature stratification in the top layer, but notice that the T-stratification is the opposite near 6–9 P.M., maybe as the result of heavy rainfall in the early night.

3.2. Individual Freshening Events

[18] A majority of the individual rainfall reports are not associated with clearly identified signals in the salinity records (except for larger high frequency variability that was commented in the previous section). On the other hand, the

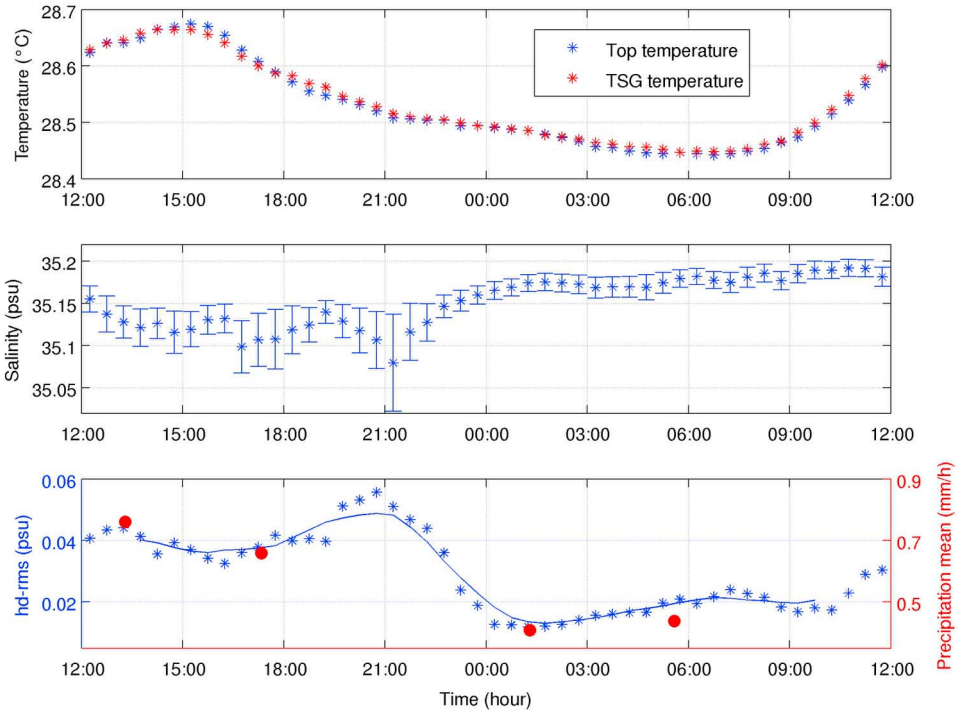

Figure 5. Same as Figure 4, but for a drifter SVP-BS 54175 under the Atlantic ITCZ often close to west Africa.

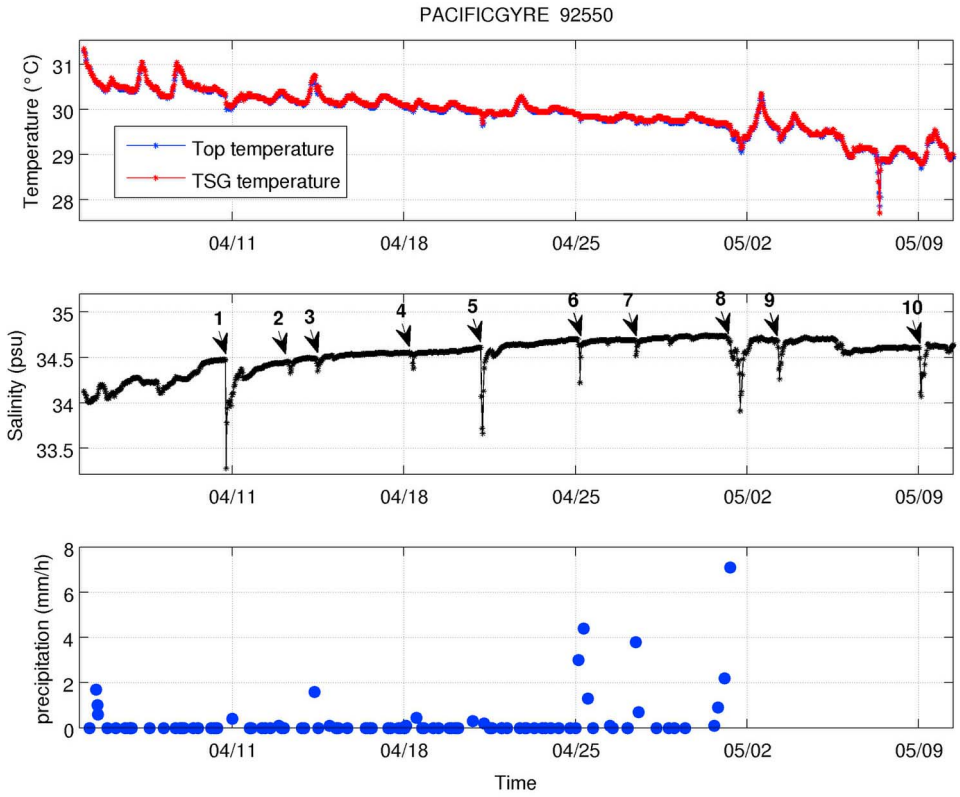

Figure 6. Time series for drifter SVP-BS 92550 in the Indian Ocean (under the ITCZ). (top) T, (middle) S, and (bottom) co-located rainfall rates. Isolated short-term drops of S are identified and numbered on the S plot (notice that some are associated with T drops). For the last part of the record, the drifter is close to an island, and thus no co-located microwave data are available.

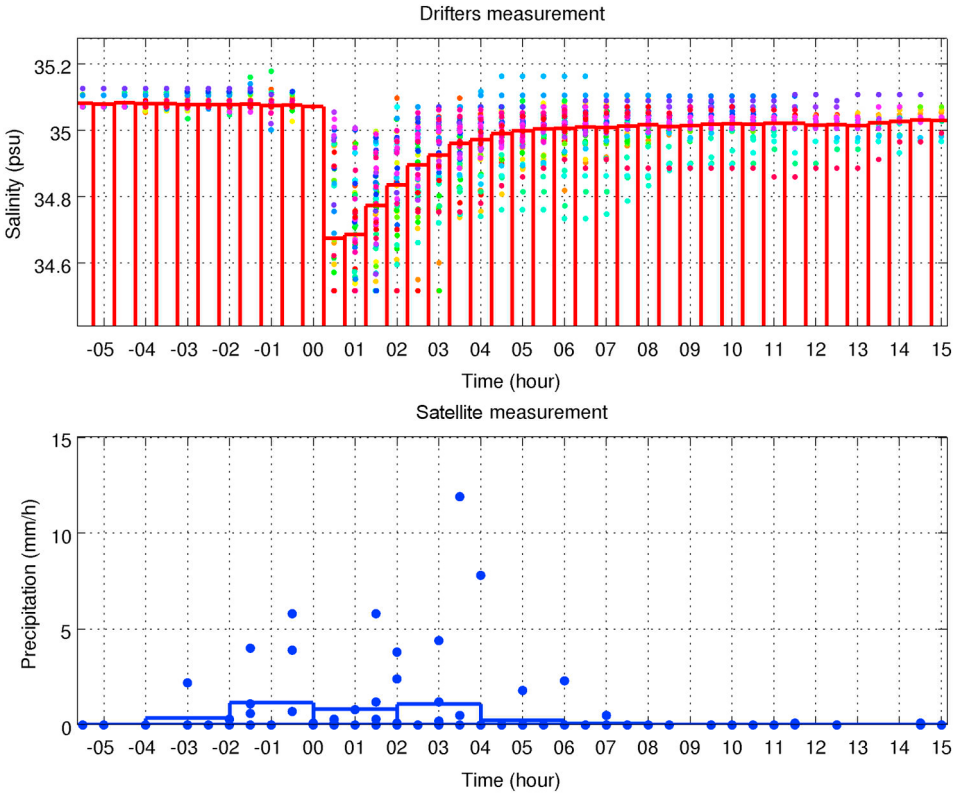

Figure 7. (top) Average cycle of salinity among 60 salinity drop events (relative to a common time of beginning of event at 00). Individual records are shifted to a common salinity value at the initial drop time. The average is plotted as well as individual events. (bottom) The associated average reported rainfall (mm/hour) plotted by 2-h average, as well as the individual values at the exact time of reports.

salinity records also present sudden drops which are a large part of the variability in the records. Some of these drops associated with a temperature change might be ocean fronts crossed by the drifter, some might be artifacts of fouling of the conductivity cell (see section 2.3 and Figure 2), but that are removed in the processing of the data, but others when there is a rapid recovery, are most likely not the result of fouling. We will thus focus on those sudden drops with rapid recovery (drops of at least 0.1 psu in less than an hour and at least 80% of the recovery within 1 day). Figure 6 illustrates the identification of such events for an Indian Ocean drifter south of the equator in the spring of 2010. Notice on this example that some of the salinity drops are also associated with temperature drops. All-together, we retain 60 such events from drifters mostly between early 2009 and March 2011.

[19] For these events, the time of minimal salinity in the drops is most commonly within 1 h after the start of the drop (with 50% with the lowest value half an hour after the beginning, 29% an hour after the beginning, and only 21% after more than an hour). The average drop is 0.56 psu, although it is highly variable with a large proportion of events (35%) in the 0.2 to 0.5 psu drop category, and 30% for drops larger than 0.5 psu, including 3 drops larger than 2 psu. There is a fast recovery after minimum salinity is reached (with an average 40% recovery within half an hour), but with a much slower recovery afterwards (75% within 5 h), and thus the records are asymmetric with respect to the salinity minimum time. We then combine the records using a common start time (beginning of the drop at time 0), refer all the records to a common initial S (or T) value, and normalize the variability in each record by the size of its drop relative to the average 0.56 psu (Figure 7). This illustrates that most of the recovery has happened 6 h after the beginning of the drop, with an average drop in this referential of 0.4 psu. There is little variability before the drop, but much more during and after (this also holds when not normalizing each event by the drop magnitude before compositing the different events). One element for this larger variability after the drop could be the wind. In particular, events with a recovery after more than 6 h (average 9 h) have average co-located wind speeds of 5.5 m/s, whereas events with recovery within less than 2 h (average 100′) have average wind speeds of 7.6 m/s. The wind would act in two ways. First, a larger wind would increase vertical mixing with the saltier subsurface water [*Price*, 1979]; second, the wind would result in a larger shear between the current at 15 m which the drifter follows, and the near surface fresh layer, thus larger relative advection with respect to the freshwater lens.

[20] Co-located rainfall data are reported (with the reference of time 0 at the beginning of the salinity drop) in Figure 7 (bottom) with averages over 2 h. Only half the reported rainfall rates are nonzero, even within an hour of the salinity drop. The total amount of rainfall on the order of 8 mm, would attribute (if concentrated over half an hour) the average drop of 0.4 psu of Figure 7 to a 70-cm surface layer.

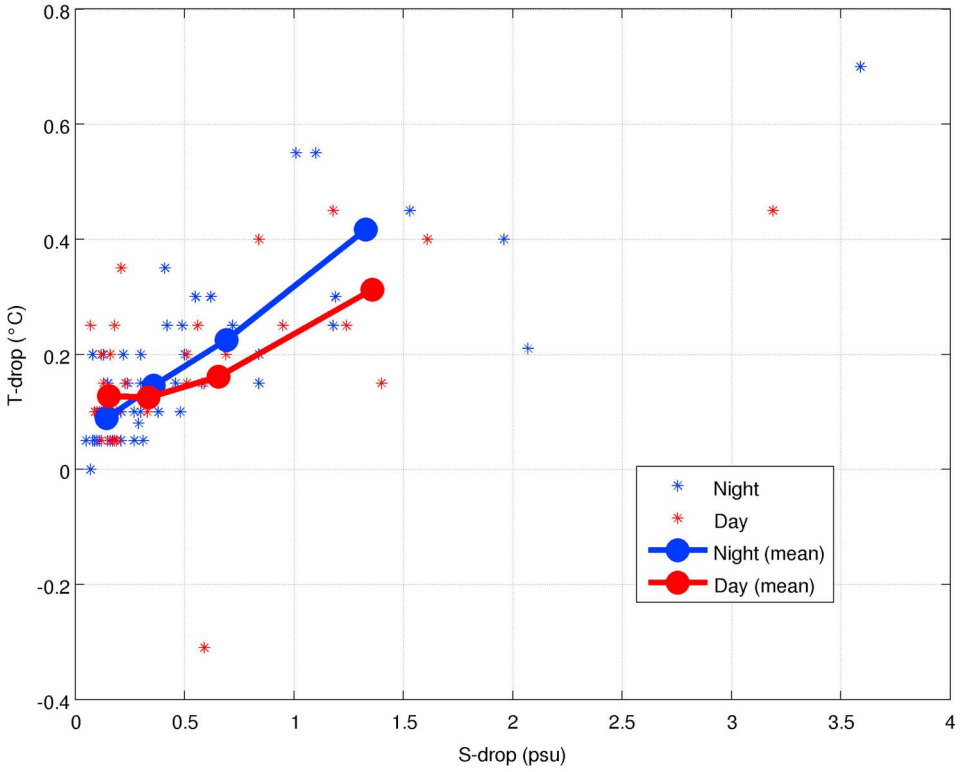

Figure 8. T-drop as a function of S-drops for individual freshening events. Blue stars for nighttime and red stars for day-time events. The lines with dots correspond to histogram values (in 0.1–0.2, 0.2–0.5, 0.5–1.0 and >1-psu categories).

With the average of individual drops of 0.56 psu, this layer would instead be only 50 cm, so just to the depth of the conductivity cell. On the other hand, the co-located reported rain lasts well after the time of minimal salinity at 50 cm, and we expect that even within the first hour of rainfall, freshwater will often penetrate by mixing deeper than 50 cm. This really implies a discrepancy between what is needed to create the observed drops and the satellite rain rates.

[21] Most of the salinity drops are associated with temperature drops. There is a large scatter between the change in temperature and the change in salinity, to some extent related to the time of the day, but also clearly to weather conditions (wind, solar irradiance…) that we cannot investigate in detail with the collocated data. A summary of it is shown in Figure 8 separating day and nighttime drop-events, where we have chosen to represent the temperature change at the time of maximum S-drop, as a function of S-drop. Except for small S-drop events, there is usually less T-decrease during day-time than nighttime, probably as a result of solar radiation warming the sea surface during day-time, although scatter is huge and the difference is not statistically significant. For small salinity drops, the T-changes remain mostly between 0.05 to 0.1°C. The time of maximum temperature drop is usually after the time of maximum salinity drop (by an average 1 h, when considering the individual events), This supports a large contribution to the temperature drops of either heat loss in the surface layer stratified by rainfall (in particular at night) [*Katsaros*, 1976] or by wind-induced stirring of a thermally stratified layer (during day time). There can be also a contribution due to cooling by raindrops (for the observed dilution, this could be up to 0.08°C [*Gosnell et al.,* 1995]; thus up to 50% of the change in T at the time of largest S-drop).

3.3. Near-Surface Stratification During Freshening Events

[22] Twenty out of the sixty freshwater events happened at times when a Surplas drifter was also providing T and S data near 15-cm depth. Comparing the two records provides information on stratification in the top 50 cm. Figure 9 illustrates the composite event. It is fairly similar (a little smaller) to the one we observed for the larger set of events used in Figure 7, and illustrates a stratification within this top 50-cm layer, both for T and S. At 15-cm depth, the S-drop is more intense and peaks earlier (within a half hour of the start) than with the 50-cm SVP-BS measurement. There is an associated T vertical gradient, which is particularly strong in the first half hour (the T-drop at 50 cm is only 45% of the drop at 15 cm). However, also in these cases, the T minimum tends to lag the S minimum by almost an hour (more pronounced at 50 cm).

[23] The stratification between the sensor levels is further illustrated by the differences in Figure 10. There is a large scatter largely due to the reported resolution and measurement accuracy, so that the T and S differences are only significant for the first half hour for S (an hour for T) following the beginning of the drop. The temperature stratification is actually a much larger proportion of the initial drop at 50 cm (55%) than is the salinity stratification (20%), and there is no clear lag between the T and S stratification, whereas there

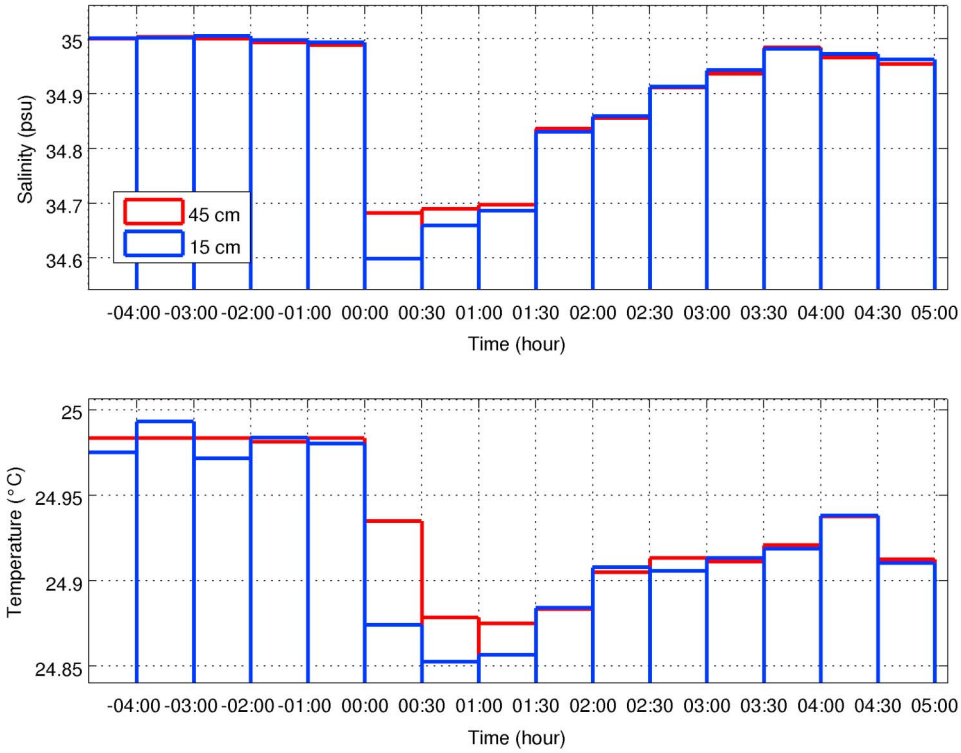

Figure 9. Average composite cycle of (top) salinity and (bottom) temperature among 20 salinity drop events observed by both SVP-BS (50 cm) and Surplas drifters (15 cm) (relative to a common time of beginning of event). Individual records are shifted to a common salinity value at the initial drop time. SVP-BS data in red and Surplas data in blue (interpolated linearly at the time of the SVP-BS measurements).

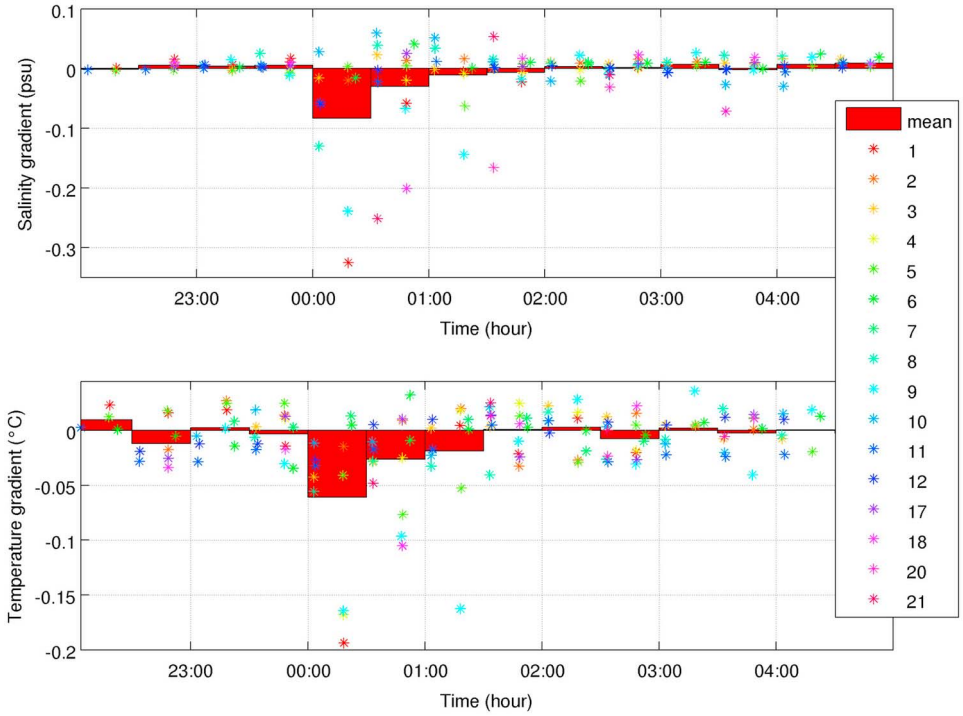

Figure 10. Difference between (top) S and (bottom) T records of the Surplas and the SVP-BS. Average histogram by half-hour and individual data (dots).

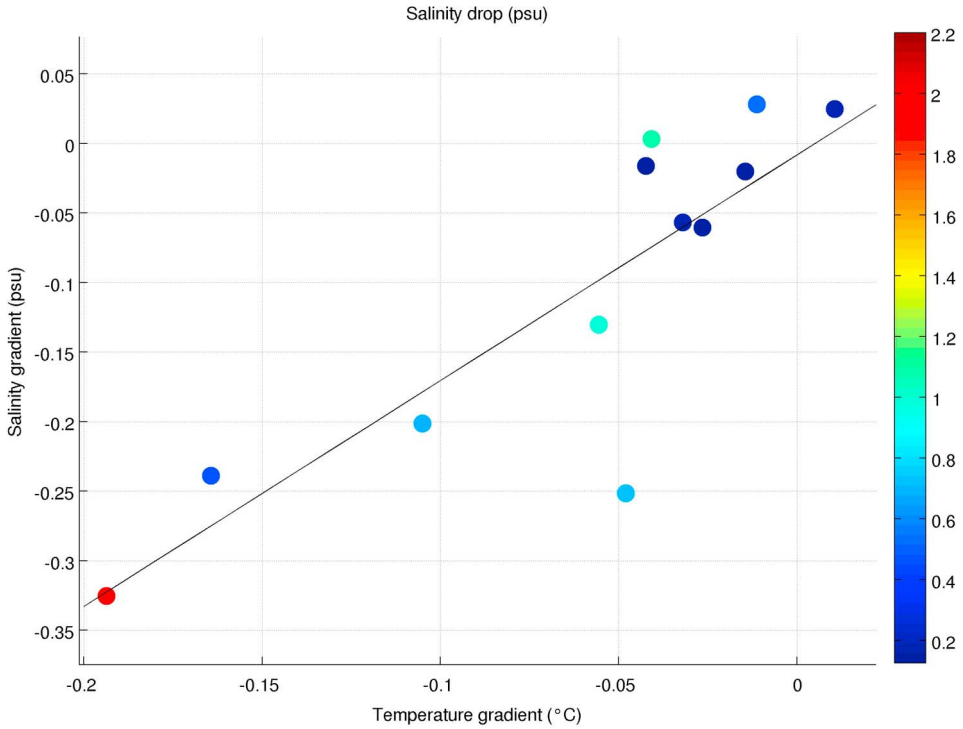

Figure 11. Scatterplot of the difference in T versus the difference in S between the Surplas and the SVP-BS records. The color is as a function of the total S-drop (right color-bar).

tended to be a lag in total signal, albeit with a dependence of T-drop on time of day, as illustrated in Figure 8. The scatterplot of T-stratification versus S-stratification (Figure 11) can be interpreted as a linear relationship between the two quantities (0.22°C for a 1% dilution). T-stratification thus reduces the initial vertical density gradient caused by S-stratification by 30%. On the other hand the amplitude of this stratification is not strongly related with the total drop magnitude.

[24] Cooling by the raindrops [*Gosnell et al.*, 1995] would contribute to a proportionality between T and S stratification (<0.05°C for a 1% dilution by freshwater). However, this would be a contribution to T-stratification less than 0.015°C for the observed S stratification; thus a smaller (<20%) contribution than for the total drop at 50 cm. The largest contribution to the initial T-stratification is thus mainly related to surface heat loss trapped in the surface layer stratified by rainfall [*Katsaros*, 1976]. As time passes and the rain event stops, vertical mixing would reduce both T and S near-surface stratifications. T then would continue to decrease under the influence of the surface heat loss counter-acting the warming due to entrainment of deeper water (at nighttime, but less so during the day), whereas S would start increasing as a result of the entrainment (and evaporation, although in a smaller proportion on these hourly time scales). Thus, the observed lag found between the largest drop in T compared to the largest drop in S is not seen in the near-surface stratification data.

[25] There is also a measurement issue associated with the initial temperature stratification, because the C and T sensors are not at the same location, which can result in errors in estimating salinity in the presence of a T gradient. However, with the T-stratification measured over the 35 cm separating the SVP-BS and the Surplas C/T measurements, the average resulting S bias could be on the order of −0.01 psu (and with the same sign for both sensors, based on errors seen for positive T-stratification at mid-day). This is thus much less than the observed S signal of the SVP-BS and the S-stratification between the two instruments.

4. Discussion and Conclusions

[26] First, we have found the use of surface salinity from drifters challenging in the tropics. This is because it is difficult to identify unambiguously erroneous parts of the records that are often associated with sudden S-jumps. Slow-varying fouling as was found in 2005 [*Reverdin et al.*, 2007] would be too small to be identified in the tropical oceans, and long-term biases cannot be corrected to better than a few 0.01 psu for those drifters. On the other hand, SVP-BS drifters are now available that provide usable salinity records for periods of up to 1 year, and with the required time-resolution to resolve the daily cycle and individual freshening events.

[27] For one long-lived drifter (SVP-BS 92546) in the southwestern tropical Pacific (centered near 165°E/11°S), right under the SPCZ in a high precipitation region, we find a well marked daily cycle of high-frequency variability of salinity closely related to the daily cycle of precipitation (maximum in late night-early morning), and only a weak associated salinity daily cycle with a suggestion of a morning minimum. The rainfall cycle fits with what is expected in this region of the SPCZ, and is similar to the one observed by *Cronin and McPhaden* [1999] at an equatorial mooring site.

On the other hand, the salinity cycle is different. At the equatorial site, the explanation for the early morning maximum in salinity was that the daily cycle was dominated by the increased vertical mixing in late night. M. McPhaden (personal communication, 2011) also suggests that similar daily cycles are found at 1M depth at other sites in the Pacific Ocean (with minima at 12 to 15 am local time).

[28] A possible contribution to the difference in daily cycles would be an influence of vertical stratification when it rains, as the TAO mooring measurements are a little deeper (at least at 1 m, with possible further influence of vertical mixing by the mooring structure). Extrapolating the salinity vertical gradient between 15 cm and 50 cm when it rains (on the order of 0.05 psu) to 1 m deep, and that it happens each time it rains 'near-by', which can reach up to 16% of the time in these high-precipitation regions [*Wentz and Spencer*, 1998], results in an average salinity gradient of 0.01 psu between the drifter and mooring levels. The daily cycle of rainfall, and thus the modulation of this vertical gradient would be of the right magnitude to wipe out at 50 cm the early morning maximum salinity seen at 1 m. There is also the possibility of a small artifact in the drifter data due to differences in the depths of the C and T measurements in presence of mid-day temperature stratification. Periods of large mid-day surface warming were removed, but we could have left a small residual positive bias in the estimated drifter S of a few 0.001 psu near 3 P.M. local time.

[29] Individual freshening events were identified in the salinity records. These are often associated with local rainfall, although the co-located radiometer rainfall was not large enough to explain the observed response. Actually, in at least half the instances, there was no microwave radiometric rainfall detected within an hour of the drop. There are two possible explanations: either the rain was really intermittent, and happened at other times, even with the at least 20 km radius of influence of the radiometric measurement. The other possibility is that some of the freshening events are not directly related to local rainfall, but are associated with freshwater pools advected relative to the drifter from further away. Such structures were observed from ship-surveys in the work by *Soloviev and Lukas* [1997]. Another point to make is that our selection to identify 'freshening events' based on the salinity records selectively favors areas with particularly large rainfall rates compared to the microwave radiometric foot-print.

[30] The SVP-BS drifter freshening events are comforted by the Surplas measurements near 15 cm attached to some of SVP-BS drifters. These data indicate near-surface stratification both in T and S during freshening events and that this upper layer is trapping some surface heat loss, thus causing a time-lag between T and S minima at 50-cm depth. The increase of S before the collocated rainfall ends also suggests that vertical mixing with the deeper than 50-cm layer happens within an hour of the beginning of the freshening. We thus expect that the freshwater content associated with the freshening event extends deeper to at least 1-m within this first hour (thus, an even larger mismatch with the estimated rainfall input of freshwater based on the co-located radiometric rainfall data of at least a factor 2). These results indicating initial near-surface stratification complement the modeling studies of *Price* [1979] indicating the propagation of the freshening signal to a deeper layer, as well as the observational statistical investigation of *Henocq et al.* [2010] for deeper freshwater stratification after rainfall, or in the study of *Wijesekera et al.* [1999] in the western equatorial Pacific Ocean.

[31] More drifter data will be necessary to investigate the averaged daily cycle and the contribution of excess late night/early morning rainfall to the SSS daily cycle in 'excess-rain' tropical regions. One year of data for drifter 92546 was actually not sufficient to extract a significant daily cycle at the expected O(0.005 psu) range [*Cronin and McPhaden*, 1999], but we suspect differences in S daily cycle between measurements from surface moorings (at 1-m depth) and at the sea surface. Nonetheless, the conclusions of this study, as well as of *Cronin and McPhaden* [1999] are that the daily cycles of near surface salinity are small. Thus, except in specific areas, the differences in salinity between early morning and evening overpasses of SMOS or Aquarius satellite missions will be very small, and certainly much smaller than uncertainties in data retrievals from L-band radiometric satellite measurements caused by incorrectly sensed daily cycle of temperature, or winds varying through the day (a 0.5°C error in afternoon-SST would typically induce a 0.05 psu error in the retrieval at 30°C; an undetected 1 m/s wind change (for 6–8 m/s) would induce a 0.4 psu error). In rain-excess regions of the deep tropics, the strong vertical stratification during freshening events, even within the top 1m of the ocean, will however remain a concern for relating the satellite retrievals to data acquired by other means, for example from 'standard' Argo floats at 5-m depth or even 1-m depth measurements from the equatorial mooring arrays.

[32] **Acknowledgments.** The drifters used in this study and the processing effort were funded by CNES for TOSCA-supported projects GLOSCAL and SMOS. Simon Morisset was funded by CNES, and the other authors by CNRS/INSU. Some of the drifters used here were also provided for GLOSCAL by CMM/CNRM, and we thank Pierre Blouch and Jean Rolland for support to the project, as well as Fabienne Gaillard for the co-ordination of the GLOSCAL project. Comments by reviewers were quite helpful.

References

Chang, A. T. C., L. S. Chiu, and G. Yang (1995), Diurnal cycle of oceanic precipitation from SSM/I data, *Mon. Weather Rev.*, *123*, 3371–3380, doi:10.1175/1520-0493(1995)123<3371:DCOOPF>2.0.CO;2.

Cravatte, S., T. Delcroix, D. Zhang, M. McPhaden, and J. LeLoup (2009), Observed freshening and warming of the western Pacific warm pool, *Clim. Dyn.*, *33*, 565–589, doi:10.1007/s00382-009-0526-7.

Cronin, M. F., and M. J. McPhaden (1998), Upper ocean salinity balance in the western equatorial Pacific, *J. Geophys. Res.*, *103*, 27,567–27,587, doi:10.1029/98JC02605.

Cronin, M. F., and M. J. McPhaden (1999), Diurnal cycle of rainfall and surface salinity in the western Pacific warm pool, *Geophys. Res. Lett.*, *26*, 3465–3468, doi:10.1029/1999GL010504.

Delcroix, T., S. Cravatte, and M. J. McPhaden (2007), Decadal variations and trends in tropical Pacific sea surface salinity since 1970, *J. Geophys. Res.*, *112*, C03012, doi:10.1029/2006JC003801.

Durack, P. J., and S. E. Wijffels (2010), Fifty-year trends in global ocean salinities and their relationship to broad-scale warming, *J. Clim.*, *23*, 4342–4362, doi:10.1175/2010JCLI3377.1.

Font, J., A. Camps, A. Borges, M. Martin-Neira, J. Boutin, N. Reul, Y. Kerr, A. Hahne, and S. Mecklenburg (2010), SMOS: The challenging sea surface salinity measurements from space, *Proc. IEEE*, *98*(5), 649–665, doi:10.1109/JPROC.2009.2033096.

Font, J., et al. (2012), SMOS first data analysis for sea surface salinity determination, *Int. J. Remote Sens.*, in press.

Gordon, A. L., and C. F. Giulivi (2008), Sea surface salinity trends over fifty years within the subtropical North Atlantic, *Oceanography*, *21*(1), 20–29, doi:10.5670/oceanog.2008.64.

Gosnell, R., C. W. Fairall, and P. J. Webster (1995), The sensible heat of rainfall in the tropical ocean, *J. Geophys. Res.*, *100*, 18,437–18,442, doi:10.1029/95JC01833.

Gruber, A., and V. Levizzani (2008), Assessment of global precipitation products, *Tech. Rep., WCRP-128*, 55 pp., World Clim. Res. Programme, Geneva, Switzerland.

Henocq, C., J. Boutin, G. Reverdin, F. Petitcolin, S. Arnault, and P. Lattes (2010), Vertical variability of near-surface salinity in the tropics: Consequences for L-band radiometer calibration and validation, *J. Atmos. Oceanic Technol.*, *27*, 192–209, doi:10.1175/2009JTECHO670.1.

Johnson, G. C., and S. E. Wijffels (2011), Ocean density change contributions to sea level rise, *Oceanography*, *24*(2), 112–121, doi:10.5670/oceanog.2011.31.

Katsaros, K. B. (1976), Effects of precipitation on the eddy exchange in a wind-driven sea, *Dyn. Atmos. Oceans*, *1*, 99–126, doi:10.1016/0377-0265(76)90009-9.

Katsaros, K. B., and K. J. K. Buettner (1969), Influence of rainfall on temperature and salinity of the ocean surface, *J. Appl. Meteorol.*, *8*, 15–18, doi:10.1175/1520-0450(1969)008<0015:IOROTA>2.0.CO;2.

Kikuchi, K., and B. Wang (2008), Diurnal precipitation regimes in the global tropics, *J. Clim.*, *21*, 2680–2696, doi:10.1175/2007JCLI2051.1.

Lagerloef, G., et al. (2010), Resolving the global surface salinity field and variations by blending satellite and in situ observation, in *Proceedings of OceanObs09: Sustained Ocean, Observations and Information for Society, Venice, Italy*, vol. 2, edited by J. Hall, D. E. Harrison, and D. Stammer, *Eur. Space Agency Publ.*, WPP-306, doi:10.5270/OceanObs09.cwp.51.

Le Vine, D., G. Lagerloef, and S. Torrusio (2010), Aquarius and remote sensing of sea surface salinity from space, *Proc. IEEE*, *98*(5), 688–703, doi:10.1109/JPROC.2010.2040550.

Lukas, R., and E. Lindstrom (1991), The mixed layer of the western equatorial Pacific Ocean, *J. Geophys. Res.*, *96*, 3343–3357.

Mignot, J., C. de Boyer-Montégut, A. Lazar, and S. Cravatte (2007), Control of salinity on the mixed layer depth in the world ocean: 2. Tropical areas, *J. Geophys. Res.*, *112*, C10010, doi:10.1029/2006JC003954.

Price, J. F. (1979), Observation of a rain-formed mixed layer, *J. Phys. Oceanogr.*, *9*, 643–649, doi:10.1175/1520-0485(1979)009<0643:OOARFM>2.0.CO;2.

Rauniyar, S. P., and K. J. E. Walsh (2011), Scale interaction of the diurnal cycle of rainfall over the maritime continent and Australia: Influence of the MJO, *J. Clim.*, *24*, 325–348, doi:10.1175/2010JCLI3673.1.

Reverdin, G., P. Blouch, J. Boutin, P. Niiler, J. Rolland, W. Scuba, A. Lourenço, and A. Rios (2007), Surface salinity measurements—COSMOS 2005 experiment in the Bay of Biscay, *J. Atmos. Oceanic Technol.*, *24*, 1643–1654, doi:10.1175/JTECH2079.1.

Roemmich, D., and the Argo Steering Team (2009), Argo: The challenge of continuing 10 years of progress, *Oceanography*, *22*(3), 46–55, doi:10.5670/oceanog.2009.65.

Schmitt, R. W. (2008), Salinity and the global water cycle, *Oceanography*, *21*(1), 12–19, doi:10.5670/oceanog.2008.63.

Soloviev, A., and R. Lukas (1997), Observation of large diurnal warming events in the near-surface layer of the western equatorial Pacific warm pool, *Deep Sea Res., Part I*, *44*, 1055–1076, doi:10.1016/S0967-0637(96)00124-0.

Sprintall, J., and M. Tomczak (1992), Evidence of barrier layer in the surface layer of the tropics, *J. Geophys. Res.*, *97*, 7305–7316, doi:10.1029/92JC00407.

Tanguy, Y., S. Arnault, and P. Lattes (2010), Isothermal mixed and barrier layers in the subtropical and tropical Atlantic Ocean during the ARAMIS experiment, *Deep Sea Res., Part I*, *57*, 501–517, doi:10.1016/j.dsr.2009.12.012.

Vialard, J., et al. (2009), CIRENE air-sea interactions in the Seychelles-Chagos thermocline ridge region, *Bull. Am. Meteorol. Soc.*, *90*, 45–61, doi:10.1175/2008BAMS2499.1.

von Schuckmann, K., and P.-Y. Le Traon (2011), How well can we derive global ocean indicators from Argo data?, *Ocean Sci.*, *7*, 783–791.

von Schuckmann, K., F. Gaillard, and P.-Y. Le Traon (2009), Global hydrographic variability patterns during 2003–2008, *J. Geophys. Res.*, *114*, C09007, doi:10.1029/2008JC005237.

Wentz, F. J., and R. W. Spencer (1998), SSM/I rain retrievals within a unified all-weather ocean algorithm, *J. Atmos. Sci.*, *55*, 1613–1627, doi:10.1175/1520-0469(1998)055<1613:SIRRWA>2.0.CO;2.

Wijesekera, H. W., C. A. Paulson, and A. Huyer (1999), The effect of rainfall on the surface layer during a westerly wind burst in the western equatorial Pacific, *J. Phys. Oceanogr.*, *29*, 612–632, doi:10.1175/1520-0485(1999)029<0612:TEOROT>2.0.CO;2.

Willis, J. K., L. M. Lyman, G. C. Johnson, and J. Gilson (2009), In situ data biases and recent ocean heat content variability, *J. Atmos. Oceanic Technol.*, *26*, 846–852, doi:10.1175/2008JTECHO608.1.

Yang, S., and E. A. Smith (2006), Mechanisms for diurnal variability of global tropical rainfall observed from TRMM, *J. Clim.*, *19*, 5190–5226, doi:10.1175/JCLI3883.1.

Yu, L. (2007), Global variations in oceanic evaporation (1958–2005): The role of the changing wind speed, *J. Clim.*, *20*(21), 5376–5390, doi:10.1175/2007JCLI1714.1.

J. Boutin, N. Martin, S. Morisset, and G. Reverdin, Laboratoire d'Océanographie et de Climatologie par Expérimentation et Analyse Numérique, Institut Pierre Simon Laplace, Université Pierre et Marie Curie, case 100, 4 pl. Jussieu, F-75252 Paris CEDEX 05, France. (gilles.reverdin@locean-ipsl.upmc.fr)